GENERALIZED DIRECTIONAL PEAK SHEAR STRESS CRITERION FOR DILATANT ROCK JOINTS

Tikou Belem, Université du Québec en Abitibi-Témiscamingue, Rouyn-Noranda, Canada
Souley Mountaka, *INERIS, LAEGO-UMERG, École des mines de Nancy, INPL, Nancy, France*
Françoise Homand, *LAEGO, École de Géologie de Nancy, INPL, Nancy, France*

ABSTRACT
A generalized directional shear strength criterion was proposed to predict the variation of peak shear stress under both constant normal stress (CNS) and variable or constant normal stiffness (CNK) loading paths for cyclic and monotonous shearing. The proposed generalized shear strength criterion was compared to the existing shear strength criteria and experimental data. The results showed the model successfully predicts the shear strength behavior of rock joints.

RÉSUMÉ
Un critère de rupture directionnelle généralisé a été proposé afin de prédire la variation de la résistance au cisaillement des joints cisaillés à contrainte normale constante (CNC) ou à rigidité normale constante (KNC) ou variable en fonction de la contrainte normale initiale (σ_{ni}), que ce soit un cisaillement monotone ou cyclique. Le critère proposé a aussi été comparé à des résultats expérimentaux et aux autres critères déjà existants. Les résultats ont montré que le modèle prédisait assez bien la résistance au cisaillement des joints rocheux.

1. INTRODUCTION

The presence of rock joints has a strong effect on the mechanical behavior and the structural stability of engineered rock structures. The behavior of rock joints under either constant normal stress (CNS) or constant normal stiffness (CNK) loading conditions depends mainly on the wall surface roughness characteristics, the degree of matching and/or interlocking of the rock surfaces, the presence of filling debris and the intact rock material properties. According to Archambault et al. (1996), the dominant factor influencing the mechanical behavior of rock joints is their morphology and roughness, and these are most difficult to characterize and model. Joint roughness will undergo continuous and progressive change during loading due to wearing, grinding, and breaking or crushing of the asperities. Many experimental results show that there is a strong correlation between the evolution of joint surface roughness and the friction properties of rock joints. Few works have been devoted to account for the progressive degradation of joint wall surface asperities during the course of monotonous or cyclic shear (e.g. Plesha 1987; Hutson and Dowding 1990; Benjelloun 1990; Jing et al. 1993; Homand et al. 1999).

The knowledge of the shear strength of rock joints is necessary to determine the stability of jointed rock masses. The variation of peak shear stress with normal stress has been modeled by many authors (Patton 1966; Ladanyi and Archambault 1969; Jagger 1971; Barton 1973; Swan and Jongqi 1985; Saeb 1990), and more recently by Kulatilake et al. (1995). Although these models have substantially improved our knowledge of the behavior of rock joints, their limitations must be recognized (Archambault et al. 1996) because they do not account for the friction variation of rock joints due to the degradation of the surface roughness. Most of the existing shear strength criteria have been formulated to predict only the peak shear stress of dilatant joints undergoing monotonous shear under constant normal stress (CNS) loading conditions. However, many authors (e.g. Leichnitz 1985; Saeb 1989; Archambault et al. 1990; Saeb and Amadei 1990) have already proposed some approaches to predict rock joint response under constant or variable normal stiffness from experimental results obtained from direct shear tests under constant normal stress loading. Among these approaches, the Saeb and Amadei's graphical method (Saeb and Amadei 1990) gives more or less satisfactory results, but the method is difficult to use.

The purpose of this paper is to predict the peak shear stress of artificial or natural rock joints by taking into account (i) the loading path (CNS or CNK), (ii) the shearing path (monotonous or cyclic), (iii) the shearing direction, (iv) the surface morphology shape (anisotropic or isotropic) and, (v) the evolution of 2nd-order roughness. Roughness is subdivided into two components in the concept of primary and secondary asperities: the secondary (or 2nd-order) and the primary (or 1^{rst}-order) roughness (Jing et al. 1993, Kana et al. 1996; Belem et al. 2000). The secondary roughness corresponds to the surface heights distribution (and denotes the *sensu stricto* roughness) while the primary roughness corresponds to the surface geometry that describes the anisotropy of its morphology. To achieve this goal, a generalized shear strength criterion is proposed which takes into account the 1^{rst}-order and 2nd-order roughness through new proposed roughness parameters defined with the aid of 3D laser profilometry (Belem et al. 2000, Belem et al. 1997, Belem 1997). The model parameters describe joint initial morphology such as the degree of 2nd-order roughness (DR_r), the joint surface or 3D mean angle (θ_s), the degree of apparent anisotropy of joint surface morphology (k_a),

the surface amplitude or maximum asperity height (a_0) and the maximum or cumulated shear displacement ($U_s^{\max}$). This approach takes into account the interlocking and dilatant nature of sheared rock joints and the shearing direction (φ). The strength behavior predicted by the proposed new generalized shear strength criterion is compared to the results of previous laboratory monotonous and cyclic direct shear tests under CNS and CNK loading conditions and to the shear strength criteria proposed by Ladanyi and Archambault (1969), Barton (1973) and Saeb (1990).

2. JOINT MORPHOLOGY PARAMETERS

Numerous new joint roughness parameters have been proposed by Belem *et al*. (2000) to supplement and overcome the inadequacy or the subjectivity of some of the existing joint linear profile parameters (*e.g*. *Z2*, R_L, P_s and *JRC*). These new proposed roughness parameters are more suitable for joint surface roughness characterization that includes different characteristics such as magnitude, angularity, and anisotropy. In this paper, only the parameters used in the generalized directional shear strength criterion are presented but more details are found in Belem et al. (2000).

2.1 Primary roughness parameters

2.1.1 Roughness profile angularity

For the entire joint surface involving identical/non-identical roughness profile lengths (e.g. circular sections), the one-directional surface profile mean angle (θ_p), defined as the weighted mean of the parameter θ^*_p, is given as follows:

$$\left(\theta_p\right)_{k=x,y} = \operatorname{atan}\left(\sum_{j=1}^{M_k} L_k^j \left(\frac{1}{N_k^j - 1} \sum_{i=1}^{N_k^j - 1} \left| \frac{z_{i+1} - z_i}{\Delta k} \right| \right) \Bigg/ \sum_{j=1}^{M_k} L_k^j \right) \quad [1]$$

where z_i is the discrete values of profile heights; Δk is the sampling step along *k*-axis; M_k is the total number of profiles in *k*-direction (*x* or *y*); N_k^j the number of discrete points corresponding to the j^{th} profile along *k*-axis; L_k^j the length of the j^{th} profile along *k*-axis. When all the surface profiles have the same nominal length Eq. [1] is reduced to an arithmetic mean.

2.1.2 Degree of apparent anisotropy

The degree of apparent anisotropy of surface morphology, k_a, can be defined as follows:

$$k_a = \frac{\min\left\{\theta_{p(x)}, \theta_{p(y)}\right\}}{\max\left\{\theta_{p(x)}, \theta_{p(y)}\right\}} \qquad \text{with } 0 \le k_a \le 1 \quad [2]$$

Subscript *x* and *y* in Eq. [2] denote respectively the direction in which the linear roughness profile weighted mean angle, θ_p, is calculated. Parameter k_a varies from 0 to 1: when k_a = 0, the surface morphology is anisotropic and exhibiting saw tooth shapes or undulations; when k_a = 1, the surface morphology is perfectly isotropic.

2.2 Secondary roughness parameters

2.2.1 Surface angularity

The three-dimensional mean angle of the entire surface is calculated by summing all of the inclination angles, θ_i, of the normal unit vectors of all the elementary surfaces as follows:

$$\theta_s = \frac{1}{N} \sum_{i=1}^{N} \theta_i \quad [3]$$

where *N* is the total number of elementary flat surfaces. Angle θ_s is considered to be the mean angle of surface asperities or surface angularity parameter.

2.2.2 Degree of surface roughness

The degree of joint surface relative roughness, DR_r, was derived from the surface roughness coefficient (R_s) defined for a single joint wall by El Soudani (1978). DR_r relates the evolution of surface roughness to its initial state by the following relationship:

$$DR_r = \frac{A_t - A_n}{A_t} = \frac{R_s - 1}{R_s} \qquad \text{with } 0 \le DR_r < 1 \quad [4]$$

Eq. [4] shows that when the fracture surface is perfectly smooth and flat then DR_r = 0 and as the fracture surface becomes rougher then $DR_r \to 1$.

3. PROPOSED FAILURE CRITERION FOR CONSTANT NORMAL LOADING PATH (CNS)

3.1 Basic assumptions

In the present approach, the authors assume that there are two main types of joints:

i) non-dilatants joints (isotropic surface morphology),

ii) dilatant joints (isotropic/anisotropic surface morphology).

The authors assume that dilatant joint surfaces (regular or irregular joints) are often anisotropic and more or less isotropic/anisotropic where the 1^{rst}-order roughness component plays a preponderant role. We also assume that non-dilatant joint surfaces (generally irregular) are more or less isotropic and only the 2nd-order roughness governs the shear strength behavior. In addition, we also assume that a dilatant joint will tend to be much less degraded than a non-dilatant joint which would be more degraded during the course of shearing. Dilatant joints are usually mated and/or interlocked while non-dilatant joints can be non-mated and non-interlocked (e.g. soil-structure, rock-structure, soil-rock, concrete-rock or mine backfill-rock interfaces).

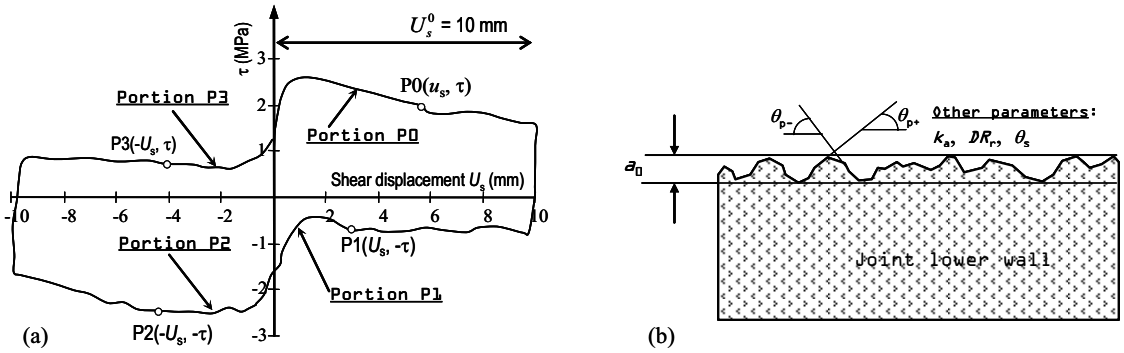

Figure 1. Shear strength model parameters: (a) typical cyclic shear curve showing the four portions; (b) morphological parameters previously defined.

The model is formulated in the more general case of cyclic shearing where the shear displacement–shear stress curve (U_s, τ) is divided into four portions (Fig. 1a). For each cycle of shearing the model will predict the peak shear stress (τ_p) on the first portion, *P0*, of the (U_s, τ) curve as shown in Fig. 1a. Shear displacement (U_s) on the portion *P0* will be U_s^0 and the shear displacement for one cycle of shearing will be of $4U_s^0$. If *n* is the number of cycles of shearing, the maximum (or cumulated) shear displacement on the portion *P0*, $U_s^{max} = U_s^0(4n - 3)$. For monotonous shearing, *n* = 1 and $U_s^{max} = U_s^0$. The model parameters will be the previously defined joint surface morphological parameters (k_a, θ_s, DR_r), as well as the characteristics of shear tests (*n*, U_s^0). Another important parameter to take into account in the model formulation is the joint surface amplitude (a_0), which is the difference between the maximum and the minimum asperity heights (Fig. 1b). Noticed that the parameter a_0 takes into account the interlocking nature of the joint samples and will govern the magnitude of dilatancy developed during the course of shearing.

3.2 Formulation of the failure criterion

It was found from previous investigations (Homand et al. 1999; Belem 1997; Lefêvre 1999) that for a moderately dilatant joint, cyclic shearing involved a progressive degradation of the joint surface roughness, which in turn increases contact areas and therefore the shear strength. Consequently, a failure criterion must take into account the "pure" dilatancy (i_{pure}), which is the combination of the observed peak dilatancy, $i_{p(exp)}$, and the asperity degradation component of dilatancy, $i_{deg.}$, as follows:

$$i_{pure} = i_p(\exp) + i_{deg.} = \delta_d^o \qquad [5]$$

Angle i_{pure} can be predicted directly which and corresponds to a dilatancy-degradation angle, $\delta_d°$ (subscript *d* denotes degradation process) for the case of joint exhibiting a moderate degradation potential. In the present approach, Barton's failure criterion (Barton 1973) was considered as the basic model from which the new model will be proposed. By replacing d_n^o in Barton's failure criterion with Eq. [5], the proposed shear strength criterion for CNS loading path is given by the following relationship:

$$\tau_p\big|_{CNS} = \sigma_n \tan\left(\phi_b + \delta_d^o\right) \qquad [6]$$

To better predict peak shear stress, the new dilatancy-degradation angle, $\delta_d°$, must be defined in order to explicitly take into account both dilatancy phenomenon and degradation of surface asperities during the course of monotonous or cyclic shearing. This new dilatancy-degradation angle must be greater than the observed peak dilatancy angle ($\delta_d° > i_p$). Based on our experimental observations (Belem 1997), the dilatancy-degradation angle, $\delta_d°$, can be formulated as follows:

$$\delta_d^o = 2\theta_s \exp\left(-\kappa\frac{\sigma_n}{\sigma_c}\right) \qquad [7]$$

where κ is a constant depending on the joint surface morphology and the number of cycles of shearing; σ_n and σ_c are normal stress and uniaxial compressive strength of the sample material.

Angle $\delta_d°$ describes the effect of dilatancy as well as the surface change due to asperities degradation which increases joint wall surface contact area and hence the shear strength. It was found that the constant κ can be expressed as follows:

$$\kappa = \frac{(1-k_a)^2}{DR_r}\frac{3a_0}{2U_s^0}\frac{1}{\log_{10}\left(\frac{U_s^{max}}{a_0}\frac{1}{n}\right)} \qquad [8a]$$

and in term of number of cycles of shearing, *n* :

$$\kappa = \frac{(1-k_a)^2}{DR_r}\frac{3a_0}{2U_s^0}\frac{1}{\log_{10}\left(\frac{U_s^0}{a_0}\frac{(4n-3)}{n}\right)} \qquad [8b]$$

Finally, the dilatancy-degradation angle, $\delta_d°$, is given as follows:

$$\delta_d^o = 2\theta_s \exp\left(-\frac{\sigma_n}{\sigma_c}\frac{3a_0}{2U_s^0}\left[\frac{(1-k_a)^2}{\log_{10}\left(\frac{U_s^0}{a_0}\frac{(4n-3)}{n}\right)DR_r}\right]\right) \quad [9]$$

where all the parameters are previously defined.

Substituting Eq. [9] into Eq. [6], the general expression for the prediction of CNS peak shear stress, taking into account the influence of dilatancy, asperities degradation and the number of cycles of shearing is given as follows:

$$\tau_p\big|_{CNS} = \sigma_n \tan\left(\phi_b + 2\theta_s \exp\left(-\frac{\sigma_n}{\sigma_c}\left[\frac{3a_0}{2U_s^0}\frac{(1-k_a)^2}{\log_{10}\left(\frac{U_s^0}{a_0}\frac{(4n-3)}{n}\right)DR_r}\right]\right)\right) \quad [10]$$

Figure 2 shows the predicted theoretical curves of peak shear stress obtained with Eq. [10] for a mortar joint with undulated surfaces.

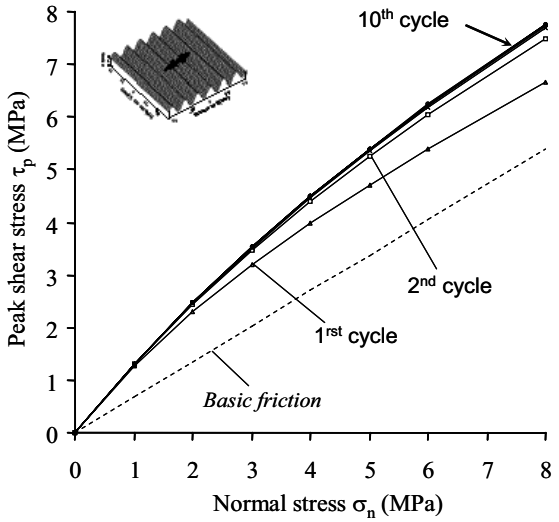

Figure 2. Theoretical cyclic shear strength curves predicted by Eq. [10] for an undulated joint (σ_c = 75 MPa, ϕ_b = 34°, θ_s = 10°, k_a = 0.21, DR_r = 0.023, a_0 = 2mm, U_s^o = 10mm, n = 10, U_s^{max} = 400mm).

3.3 Directional failure criterion

Depending on the shape of the joint surfaces, the peak shear stress will depend on the shearing direction angle (φ). The directional shear strength criterion is then given by the following equation:

$$\tau_p(\varphi)\big|_{CNS} = \sigma_n \tan\left(\phi_b + \delta_d^o(\varphi)\right) \quad [11]$$

where $\delta_d°(\varphi)$ is the directional dilatancy-degradation angle obtained for a given shearing direction, φ(in degree).

The directional dilatancy-degradation angle, which depends on the degree of apparent anisotropy, is given by the following relationship:

$$\delta_d^o(\varphi) = \delta_d^o * \cos\left(\varphi(1-k_a)\right) \quad [12]$$

where k_a is the degree of apparent anisotropy; φ is the shearing direction.

Substituting Eq. [12] into Eq. [11] yield the directional peak shear stress for dilatant joints underwent monotonous or cyclic shearing under constant normal loading path which is given as follows:

$$\tau_p(\varphi)\big|_{CNS} = \sigma_n \tan\left(\phi_b + \delta_d^o * \cos\left[\varphi(1-k_a)\right]\right) \quad [13]$$

where $\delta_d°$ is given by Eq. [9].

Figure 3 shows the predicted directional peak shear stress curves for a mortar joint with undulated surfaces after one cycle (first cycle) of shearing. Noticed that the zero direction (φ = 0°) corresponds to the direction perpendicular to the joint surface undulations and the 90° direction (φ = 90°) corresponds to the direction parallel to the joint surface undulations.

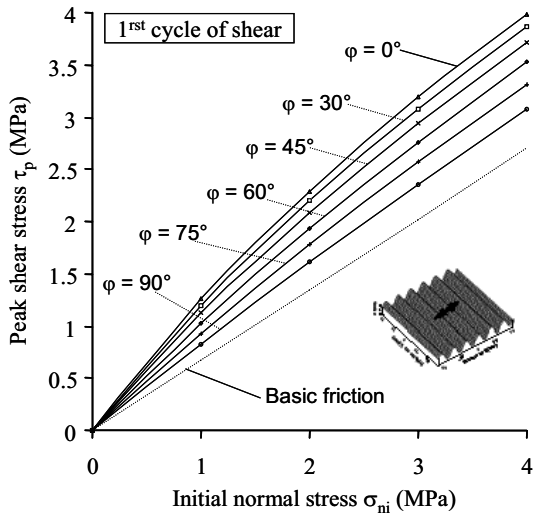

Figure 3. Theoretical directional shear strength curves predicted by Eq. [13] for an undulated joint (σ_c = 75 MPa, ϕ_b = 34°, θ_s = 10°, k_a = 0.21, DR_r = 0.023, a_0 = 2mm, U_s^o = 10mm, n = 1, U_s^{max} = 40mm).

4. GENERALIZED DIRECTIONAL FAILURE CRITERION FOR DILATANT JOINTS

The existing shear strength criteria are formulated to only predict the shear strength under CNS loading path. During shearing the normal stiffness, K = 0 for CNS loading while K > 0 for CNK loading (σ_n > 0 and constant for CNS loading, while σ_n varies continuously from its initial value in the course of shearing for CNK loading). The normal stiffness, K, is related to the normal stress, σ_n, and the normal displacement (or dilatancy, U_n) as follows:

$$K = \frac{d\sigma_n}{dU_n} = \lim_{\Delta u_n \to 0} \frac{\Delta\sigma_n}{\Delta U_n} \qquad [14a]$$

and

$$\begin{cases} \Delta\sigma_n = \sigma_n - \sigma_{ni} = K \cdot \Delta U_n \\ \sigma_n = \sigma_{ni} + K \cdot \Delta U_n \end{cases} \qquad [14b]$$

where σ_{ni} is the initial normal stress.

Since we want to predict the peak shear stress, then only the peak dilatancy (U_{np}) will be considered ($\Delta U_n \approx \Delta U_{np}$). The variation of peak dilatancy is related to the peak dilatancy rate, $\tan(i_{p^*})$, and the incremental shear displacement, ΔU_s, by the following relationship:

$$\Delta U_{np} = \Delta U_s \tan(i_{p^*}) \qquad [15]$$

As only the first portion (*P0*) of the shear curve is concerned (see Fig. 1a) for the prediction of peak shear stress, ΔU_s can reasonably be approximated by U_s^0, the shear displacement on the first portion ($\Delta U_s \approx U_s^0$). Hence, Eq. [15] becomes:

$$\Delta U_{np} = U_s^0 \tan(i_{p^*}) \qquad [16]$$

Substituting Eq. [16] into Eq. [14b] yields:

$$\sigma_{np} = \sigma_{ni} + K \cdot U_s^0 \tan(i_{p^*}) \qquad [17]$$

where σ_{np} is the normal stress value when the peak shear stress is reached during the course of shearing under CNK loading path.

From the proposed shear strength criterion for CNS loading path given by Eqs. [6, 10 & 13], a generalized shear strength criterion can be derived for both CNS and CNK loading conditions by substituting Eq. [17] into Eq. [6] as follows:

$$\tau_p\big|_{gen} = \sigma_{np} \tan\left(\phi_b + \delta_d^o\right) = \tau_p(\sigma_{ni}, K) \qquad [18a]$$

$$\tau_p(\sigma_{ni}, K) = \left(\sigma_{ni} + K \cdot U_s^0 \tan(i_{p^*})\right) \tan\left(\phi_b + \delta_d^o\right) \qquad [18b]$$

$$\tau_p(\sigma_{ni}, K) = \overbrace{\sigma_{ni} \tan(\phi_b + \delta_d^o)}^{\text{CNS loading}} + \overbrace{K \cdot U_s^0 \tan(i_{p^*}) \tan(\phi_b + \delta_d^o)}^{\text{CNK loading}} \qquad [18c]$$

The generalized directional shear strength criterion is obtained by substituting Eq. [17] into Eqs. [11 & 13] as follows:

$$\tau_p(\varphi)\big|_{gen} = \sigma_{np} \tan\left(\phi_b + \delta_d^o * \cos\left[\varphi(1 - k_a)\right]\right) \qquad [19a]$$

$$\tau_p(\varphi)\big|_{gen} = \tau_p(\sigma_{ni}, K, \varphi) = \left(\sigma_{ni} + K \cdot U_s^0 \tan(i_{p^*})\right) * \tan\left(\phi_b + \delta_d^o * \cos\left[\varphi(1 - k_a)\right]\right) \qquad [19b]$$

$$\tau_p(\sigma_{ni}, K, \varphi) = \overbrace{\sigma_{ni} \tan(\phi_b + \delta_d^o * \cos\left[\varphi(1 - k_a)\right])}^{\text{CNS loading}} + \overbrace{K \cdot U_s^0 \tan(i_{p^*}) \tan(\phi_b + \delta_d^o * \cos\left[\varphi(1 - k_a)\right])}^{\text{CNK loading}} \qquad [19c]$$

In Eqs. [18c] & [19c], the first terms of the right member correspond to the CNS loading path and the second terms correspond to the CNK loading contribution. Preliminary versions of Eq. [18] were recently introduced by the authors (Homand et al. 2001; Belem et al. 2002). When *K* = 0, Eq. [19] predicts the directional peak shear stress of CNS loading path and when *K* > 0, Eq. [19] predicts the peak shear stress of CNK loading path. From Eq. [6], Eq. [19] can be rewritten as follows:

$$\tau_p(\sigma_{ni}, K, \varphi) = \tau_p(\varphi)\big|_{CNS} * \left(1 + \frac{K \cdot U_s^0}{\sigma_{ni}} \tan(i_{p^*})\right) \qquad [20]$$

Eq. [20] clearly shows that the peak shear stress of CNK loading path can be predicted from the peak shear stress obtained under the CNS loading path (τ_{p_CNS}) either from direct shear tests or from a calculation with Eq. [13] and knowing the CNK peak dilatancy angle, i_{p^*}. Indeed, in Eq. [20] only i_{p^*} is difficult to obtain without doing any experiment. To make this generalized failure criterion practical, it is necessary to propose a relationship to predict the CNK peak dilatancy angle, i_{p^*}. It was found from our experiments (Belem 1997; Lefêvre 1999) that for a given σ_{ni}, the observed peak dilatancy angle for the CNS loading (i_p) is always greater than the peak dilatancy angle for the CNK loading (i_{p^*}) due to the effect of the normal stiffness *K*. The CNK peak dilatancy angle, i_{p^*}, can be predicted by the following exponential model:

$$i_{p^*} = \theta_s \exp\left(-\kappa' \frac{K \cdot U_s^0}{\sigma_c} \sqrt{\frac{\sigma_{ni}}{\sigma_c}}\right) \qquad [21]$$

where κ' is a constant depending on the joint surface morphology and the number of cycles of shearing. The constant κ' is given as follows:

$$\kappa' = \frac{32\left(1 - k_a - DR_r\right)^2}{DR_r} \left(\frac{a_0}{U_s^0}\right)^4 \frac{4}{\log_{10}\left(\frac{U_s^0}{a_0} \frac{(4n-3)}{n}\right)} \qquad [22]$$

Substituting Eq. [22] into Eq. [21] yields:

$$i_{p^*} = \theta_s \exp\left(-\frac{K \cdot U_s^0}{\sigma_c} \sqrt{\frac{\sigma_{ni}}{\sigma_c}} \left\{ \frac{32\left(1 - k_a - DR_r\right)^2}{DR_r} \left(\frac{a_0}{U_s^0}\right)^4 \frac{4}{\log_{10}\left(\frac{U_s^0}{a_0} \times \frac{(4n-3)}{n}\right)} \right\}\right) \qquad [23]$$

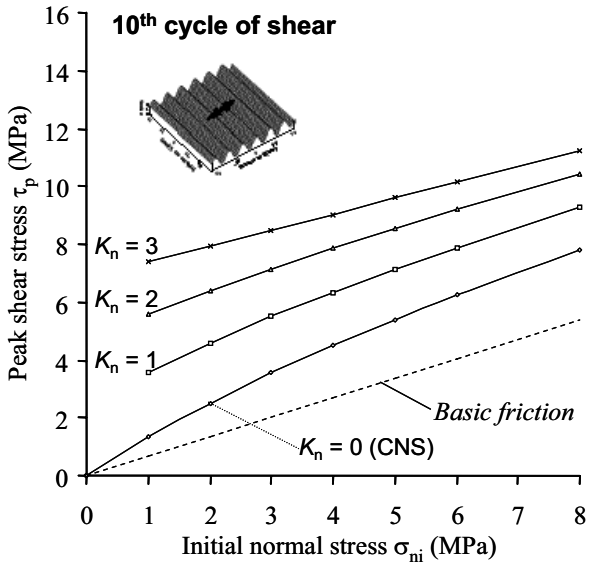

Figure 4. Theoretical cyclic shear strength curves predicted by Eq. [18] for an undulated joint sheared under CNK loading path at three different K values (σ_c = 75 MPa, ϕ_b = 34°, θ_s = 10°, k_a = 0.21, DR_r = 0.023, a_0 = 2mm, U_s^o = 10mm, n = 10, U_s^{max} = 400mm).

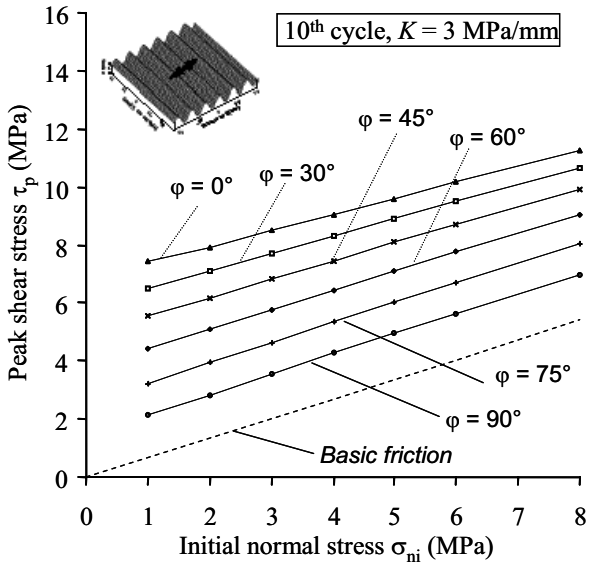

Figure 5. Theoretical directional shear strength curves predicted by Eq. [19] for an undulated joint sheared under CNK loading path at K value of 3 MPa/mm (σ_c = 75 MPa, ϕ_b = 34°, θ_s = 10°, k_a = 0.21, DR_r = 0.023, a_0 = 2mm, U_s^o = 10mm, n = 10, U_s^{max} = 400mm).

Figure 4 shows the predicted peak shear stress curves for a mortar joint with undulated surfaces after ten cycles of shearing under constant normal stiffness (CNK) loading path at a *K* value of 2 MPa/mm.

Figure 5 shows the predicted directional peak shear stress curves for a mortar joint with undulated surfaces after one cycle (first cycle) of shearing under CNK loading path at *K* value of 3 MPa/mm. Again, the direction φ = 0° is the one perpendicular to the joint surface undulations and the direction φ = 90° is the one parallel to the joint surface undulations.

5. APPLICATION OF THE PROPOSED CRITERION TO EXPERIMENTAL DATA

In order to verify the proposed generalized directional shear strength criterion (Eq. [19]), monotonous and cyclic direct shear tests were performed on two types of dilatant joints: a natural rough schist joint mortar replica and a man-made undulated mortar joint (Belem et al. 2002). The man-made undulated joints underwent 10 cycles of shearing and the natural schist joint replicas underwent monotonous shearing. Tests were performed under CNS loading path with normal stress σ_n ranging from 0.3–6 MPa and the shearing direction φ = 0°, while the CNK tests were performed at *K* values ranging from 0.16–2 MPa/mm and σ_{ni} ranging from 0.4–2 MPa.

Figure 6 presents the CNS peak shear stress predicted by the proposed generalized directional shear strength criterion (Eq. [19]) for the undulated mortar joint. From this figure there is very good agreement between observed and predicted data.

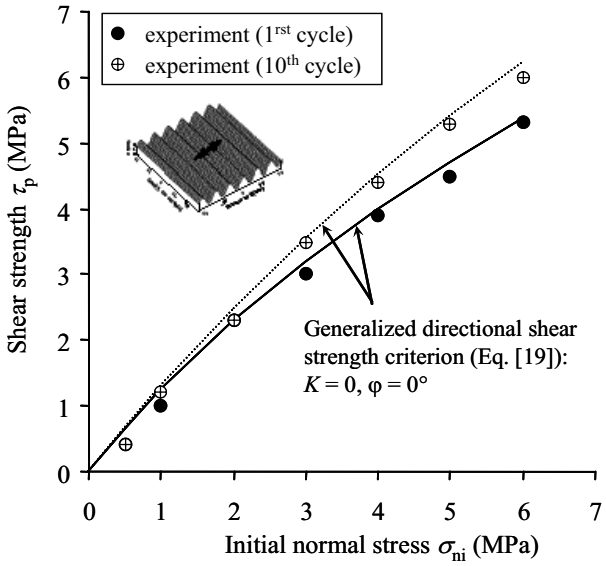

Figure 6. CNS loading path peak shear stress predicted by Eq. [19] for the regularly undulated mortar joint (σ_c = 75 MPa, ϕ_b = 34°, θ_s = 10°, k_a = 0.21, DR_r = 0.023, a_0 = 2mm, U_s^o = 10mm, n = 10, U_s^{max} = 400mm).

Figure 7 presents the observed peak shear stress of the natural schist joint mortar replica (Figure 7b) and the undulated mortar joint (Figure 7a) compared with the generalized directional shear strength criterion (Eq. [19]), and Barton (1973), Ladanyi & Archambault (1969) and Saeb (1990) shear strength criteria. One can observed that Eq. [19] is in good agreement with the observed data.

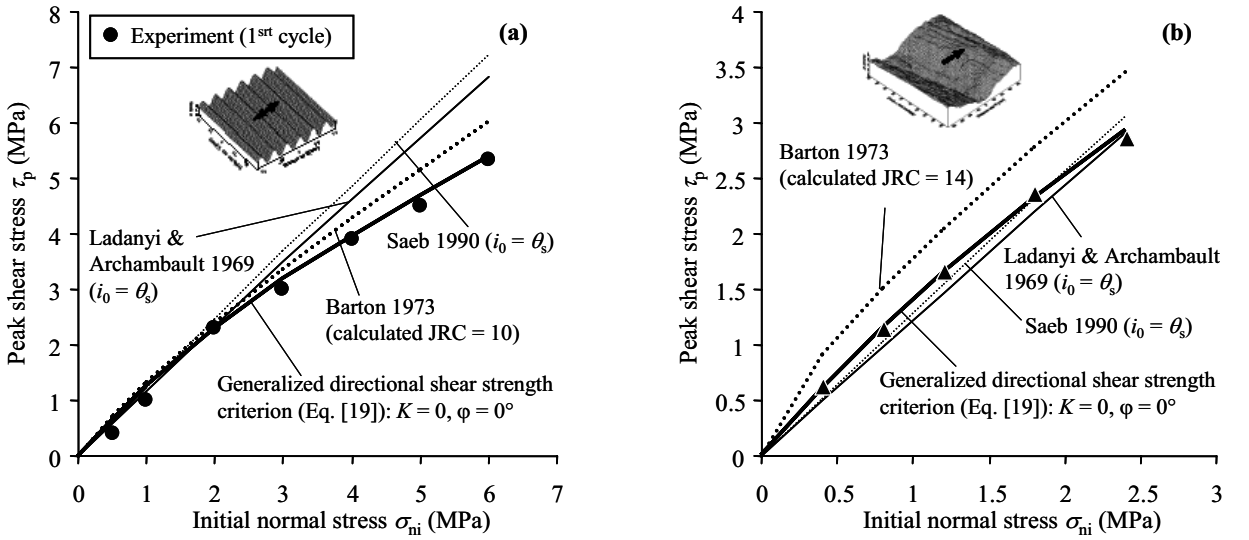

Figure 7. Comparison of the CNS loading path shear test results and the peak shear stress predicted by three shear strength criteria and compared to the generalized directional shear strength criterion (Eq. [19]: (a) for the undulated mortar joint; (b) for the natural schist joint mortar replica (σ_c = 75 MPa, ϕ_b = 34°, θ_s = 12°, k_a = 0.43, DR_f = 0.045, a_0 = 8.7mm, U_s^o = 20mm, n = 1/4, U_s^{max} = 20mm).

Figure 7 also shows that the three other failure criteria overestimate the peak shear stress of the undulated joint (Figure 7a), while for the schist joint replica the Barton's criterion overestimates peak shear stress contrary to Ladanyi & Archambault's and Saeb's criteria which slightly underestimate the joint shear strength (Figure 7b).

Figure 8 compares the CNK test results obtained on the undulated schist joint mortar replicas at two initial normal stress (σ_{ni} = 2 and 3 MPa) and normal stiffness (K = 1 and 2 MPa/mm). A good agreement between Eq. [19] prediction and experimental data is observed.

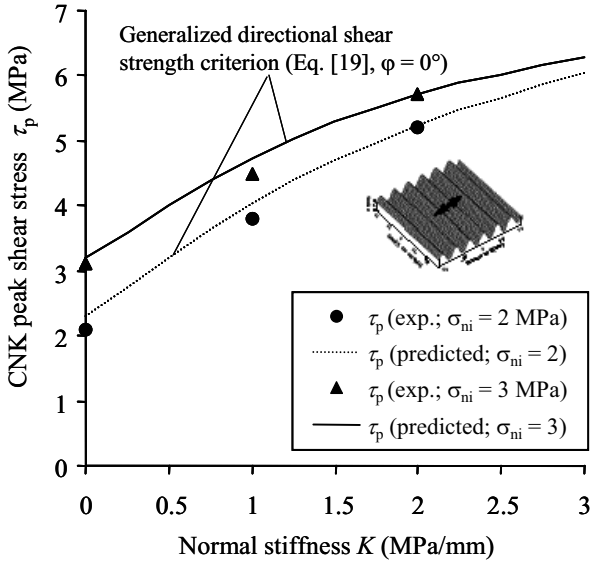

Figure 8. Comparison of the CNK loading path test results and the predicted curves by Eq. [19] for the undulated mortar joint.

6. DISCUSSION

The Barton's criterion is not in good agreement with the observed data even if the JRC values are obtained from the joint roughness profiles *Z2* values. Good agreement between the Barton's criterion and the experimental data is observed by using either back-calculated JRC value from the low normal stress (σ_n = 0.4 – 0.5 MPa) peak dilatancy angle or fictitious JRC values. This is a limitation of the Barton's criterion compared to the proposed generalized directional shear strength criterion which uses initial fixed values corresponding to the test sample properties and shear test characteristics. The efficiency of Barton's criterion depends mainly on the single JRC value, which is very difficult to accurately determine due to the subjectivity in its definition. Even if the Barton's criterion is widely used worldwide because of its simplicity and ease of use, the model's prediction capacity is diminished due to the empirical nature of JRC. The usefulness of this generalized directional shear strength criterion (Eq. [19]) is its ability to account for the cyclic shear behavior of the rock joint. Currently, the authors know of only one shear strength model which is able to quantify the effects of cyclic shearing and the shearing direction.

7. CONCLUSION

Based on surface roughness parameters previously defined by the authors (see Belem et al. 2000), a generalized directional shear strength criterion was proposed to predict moderate to marked dilatant shear strength behavior ($\tau_p(\sigma_{ni}, K, \varphi)$) of rock joints under both constant normal stress (CNS) and variable or constant normal stiffness (CNK) loading paths for monotonous and cyclic shearing. This model successfully predicted the

CNS and CNK shear strength of tested samples. The efficiency of the proposed shear strength criterion is due to the fact that the model takes into account (i) joint initial morphological parameters (k_a, θ_s, DR_r, a_0), (ii) shearing characteristics (U_s°, *n cycles,* φ) and, (iii) joint material properties (ϕ_b, σ_c).

8. ACKNOWLEDGMENTS

This work was initiated at the LAEGO Laboratory in France. Part of this research has been financed through grants from NSERC. This financial support is gratefully acknowledged.

9. REFERENCES

Archambault G, Flammang R, Riss J, Sirieix C. Joint shear behaviour revised on the basis of morphology 3D modelling and shear displacement. In Aubertin M, Hassani F, Mitri H, editors. Rock Mechanics. Rotterdam: Balkema, 1996. p. 1223–1230.

Archambault G, Fortin M, Gill D, Aubertin M, Ladanyi B. Experimental investigations for an algorithm simulating the effect of variable normal stiffness on discontinuities shear strength. Proc Int Symp Rock Joints, Loen Norway, 1990. p. 141–148.

Barton NR. Review of a new shear strength criterion for rock joint deformation. Engineering Geology 1973;7:287–332.

Belem T., Homand F. Souley M. Peak shear strength criteria for rock joint taking into account the surface isotropy and anisotropy. In Hammah R., Bawden W., Curran J. and Telesnicki M. editors. Proc. 5th NARMS and the 17th TAC Conference (NARMS-TAC 2002): "Mining and tunneling innovation and opportunity", July 07-10, Toronto, Canada, 2002. Univ. of Toronto Press, Vol. 1: pp. 45–52.

Belem T, Homand F, Souley M. Quantitative parameters for rock joint surface roughness. Rock Mech Rock Engng 2000;33(4):217–242.

Belem T, Homand-Etienne F, Souley M. Fractal analysis of shear joint roughness. Int J Rock Mech & Min Sci 1997;34(3-4), paper No. 130.

Belem T. Morphology and mechecanical behavior of rock discontinuities (in french). PhD thesis, Institut National Polytechnique de Lorraine, France, 1997. 220p.

Benjelloun ZH, Boulon M, Billaux D. Experimental and numerical investigation on rock joints. In Barton N, Stephansson O editors. Rock Joints. Rotterdam: Balkema, 1990. p. 171–178.

El Soudani SM. Profilometric analysis of fractures. Metallography 1978;11:247–336.

Homand F, Belem T, Souley M. Friction and degradation of rock joint surfaces under shear loads. Int J Numer Anal Meth Geomech 2001;25:973–999.

Homand-Etienne F, Lefêvre F, Belem T, Souley M. Rock joints behavior under cyclic direct shear tests. In Amadei B, Kranz RL, Scott GA, Smeallie PH editors. Proc 37th US Rock Mechanics Symp, Vail, Colorado, 1999. p. 399–406.

Hutson RW, Dowding CH. Joint asperity degradation during cyclic shear. Int J Rock Mech Min Sci & Geomech Abstr 1990;27(2):109–l119.

Jaegger JC. Friction of rocks and stability of rock slopes. Geotechnique, 1971;21(2):97–134.

Jing L, Nordlund E, Stephansson O. Study of rock joints under cyclic loading conditions. Rock Mech Rock Engng 1993;26(3):215–232.

Kana DD, Fox DJ, Hisiung SM. Interlock/friction model for dynamic shear response in natural jointed rock. Int J Rock Mech Min Sci & Geomech Abstr 1996;33(4):371–386.

Kulatilake PHSW, Shou G, Huang TH, Morgan RM. New peak shear strength criteria for anisotropic rock joints. Int J Rock Mech Min Sci and Geomech Abstr 1995;32(7):673–697.

Ladanyi B, Archambault G. Simulation of the shear behaviour of a jointed rock mass. Proc 11tht Symp on Rock Mech, Berkeley, 1969. p. 105–125.

Lefêvre F. Comportement mécanique et morphologique des discontinuités en cisaillement. PhD thesis, Institut National Polytechnique de Lorraine, France, 1999. 144p.

Leichnitz W. Mechanical properties of rock joints. Int J Rock Mech Min Sci and Geomech Abstr 1985;22:217–242.

Patton FD. Multiple modes of shear failure in rock. Proc 1rst Congr Int Soc Rock Mech, Lisbon, 1966. p. 509–513.

Plesha ME. Constitutive models for rock discontinuities with dilatancy and surface degradation. Int J for Num and Anal Meth in Geom 1987;11:345–362.

Saeb S, Amadei B. Modelling joint response under constant or variable normal stiffness boundary conditions. Int J Rock Mech Min Sci and Geomech Abstr 1990;27:213–217.

Saeb S. A variance on Ladanyi and Archambault's shear strength criterion. In Barton N, Stephansson O editors. Rock Joints. Rotterdam: Balkema, 1990. p. 701–705.

Saeb S. Effect of boundary conditions on the shear behavior of a dilatant rock joint. Proc 30th US Symp on Rock Mech, Univ of Colorado, 1989. p. 107–114.

Swan G, Zongqi S. Prediction of shear behaviour of joints using profiles. Rock Mech and Rocks Engng 1985;18:183–212.